Article

The Mechanism Responsible for Extraordinary Cs Ion Selectivity in Crystalline Silicotitanate

Aaron J. Celestian, James D. Kubicki, Jonathon Hanson, Abraham Clearfield, and John B. Parise

J. Am. Chem. Soc., **2008**, 130 (35), 11689-11694 • DOI: 10.1021/ja801134a • Publication Date (Web): 07 August 2008

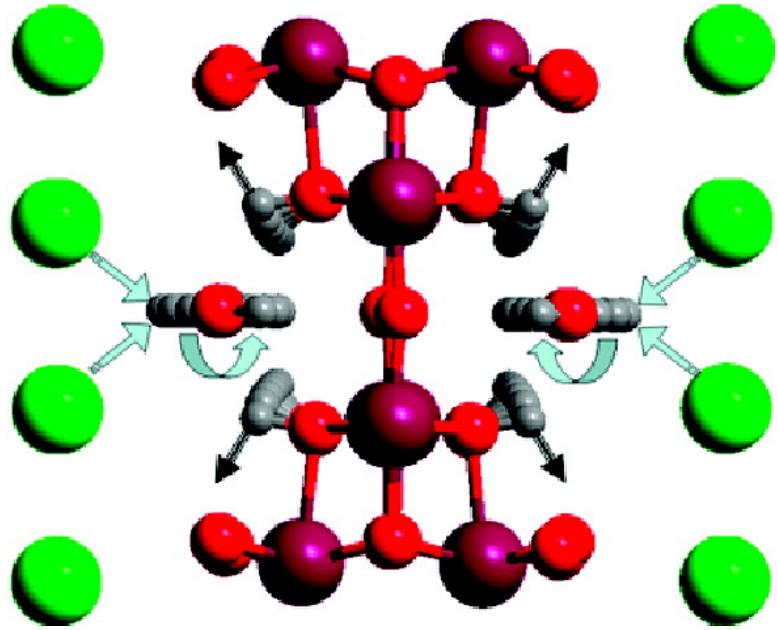

J|A|C|S
ARTICLES

Published on Web 08/07/2008

The Mechanism Responsible for Extraordinary Cs Ion Selectivity in Crystalline Silicotitanate

Aaron J. Celestian,*,† James D. Kubicki,‡ Jonathon Hanson,§ Abraham Clearfield,|| and John B. Parise⊥

Materials Characterization Center, Department of Geography and Geology, Western Kentucky University, Bowling Green, Kentucky 42101-1066, Center for Environmental Kinetics Analysis, Department of Geosciences, Pennsylvania State University, University Park, Pennsylvania 16802, Chemistry Department, Brookhaven National Laboratory, Upton, New York 11973-5000, Department of Chemistry, Texas A&M University, College Station, Texas 77842, and Center for Environmental and Molecular Sciences, Departments of Geosciences and Chemistry, Stony Brook University, Stony Brook, New York 11794-2100

Received February 20, 2008; E-mail: aaron.celestian@wku.edu

Ⓦ **This paper contains enhanced objects available on the Internet at http://pubs.acs.org/jacs.**

Abstract: Combining information from time-resolved X-ray and neutron scattering with theoretical calculations has revealed the elegant mechanism whereby hydrogen crystalline silicotitanate (H-CST; $H_2Ti_2SiO_7 \cdot 1.5H_2O$) achieves its remarkable ion-exchange selectivity for cesium. Rather than a simple ion-for-ion displacement reaction into favorable sites, which has been suggested by static structural studies of ion-exchanged variants of CST, Cs^+ exchange proceeds via a two-step process mediated by conformational changes in the framework. Similar to the case of ion channels in proteins, occupancy of the most favorable site does not occur until the first lever, cooperative repulsive interactions between water and the initial Cs-exchange site, repels a hydrogen lever on the silicotitanate framework. Here we show that these interactions induce a subtle conformational rearrangement in CST that unlocks the preferred Cs site and increases the overall capacity and selectivity for ion exchange.

Introduction

Understanding the underlying atomistic mechanisms responsible for a material's functionality is considered a prerequisite for establishing methodologies to modify its properties. The well-known selectivity accompanying conformational changes in proteins is an excellent example of how nature fine-tunes structure for functionality.[1–3] Such conformational transformations are rare in engineered inorganic systems. When they do occur, elucidation of the mechanism can provide hope that biological-like functionality in terms of selectivity might be possible. Porous inorganic ion exchangers, such as naturally occurring zeolites and clays,[4,5] provide numerous examples of selective cation removal. Materials with exceptional selectivity are studied with an eye to the strategy stated above: the exchange mechanisms are identified, and then crystal structures are targeted for modification, which leads to the synthesis of new materials with improved physicochemical properties. Hydrogen crystalline silicotitanate (H-CST; $H_2Ti_2SiO_7 \cdot 1.5H_2O$) with the mineral sitinakite topology[4,6] provided a textbook example of this approach.

The selectivity of CST for Cs^+, even in highly alkaline solutions of 1−7 M NaOH and $NaNO_3$,[7] and the physicochemical resistance of CST to crystalline deterioration by both strong radiation fields and high-pH (>12) solutions make this material capable of high-level radioactive waste sequestration. Removal of ^{137}Cs and ^{90}Sr from nuclear waste solutions is required for the safe transport and long-term storage of these solutions because of their emission of penetrating γ-radiation.[5,8] The potential for release of environmentally toxic metals has prompted the development of strategic engineering routes for new crystalline compounds that selectively absorb harmful species while resisting any deteriorative side effects themselves. In addition, the viability of the U.S. nuclear energy program is hindered by the inability to store spent nuclear fuel safely and securely for at least 10,000 years, as mandated by the U.S. Nuclear Regulatory Commission. This need has forced the development of new materials to safely store high-level waste for millennia. Regardless of which materials are selected for

† Western Kentucky University.
‡ Pennsylvania State University.
§ Brookhaven National Laboratory.
|| Texas A&M University.
⊥ Stony Brook University.

(1) Doyle, D. A.; Carbral, J. M.; Pfuetzner, R. A.; Kuo, A.; Gulbis, J. M.; Cohen, S. L.; Chait, B. T.; MacKinnon, R. *Science* **1998**, *280*, 69–77.
(2) MacKinnon, R. *Nature* **1991**, *350*, 232–235.
(3) Long, S. B.; Tao, X.; Campbell, E. B.; MacKinnon, R. *Nature* **2007**, *450*, 376–382.
(4) Clearfield, A. *Solid State Sci.* **2001**, *3*, 103–112.
(5) Sylvester, P.; Behrens, E. A.; Graziano, G. M.; Clearfield, A. *Sep. Sci. Technol.* **1999**, *34*, 1981–1992.
(6) Menshikov, Y. P.; Sokolova, E. V.; Yegorov-Tismenko, Y. K.; Khomyakov, A. P.; Polezhaeva, L. I. *Zap. Vseross. Mineral. Ova.* **1992**, *121*, 94–99.
(7) Zheng, Z. X.; Gu, D.; Anthony, R. G.; Klavetter, E. *Ind. Eng. Chem. Res.* **1995**, *34*, 2142–2147.
(8) Fiskum, S. K.; Blanchard, D. L.; Arm, S. T.; Peterson, R. A. *Sep. Sci. Technol.* **2005**, *40*, 51–67.

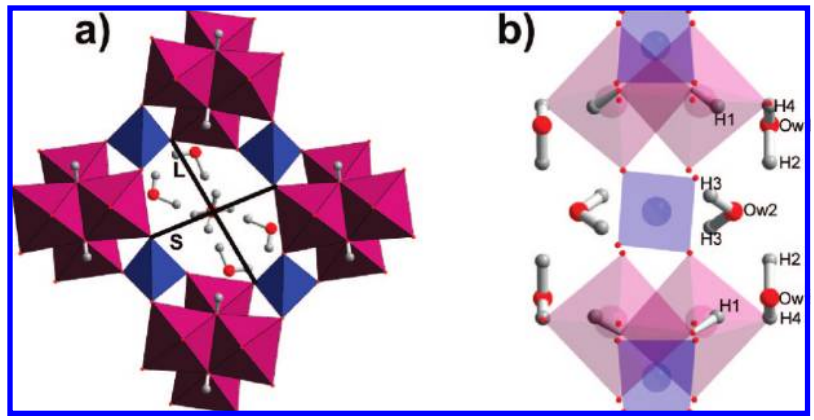

Figure 1. Polyhedral representation of the H-CST framework. (a) View of H-CST 8MR channels along [001]. Only H_2O is in the 8MR channels. For the H-CST 8MR, L/S = 1.53. (b) Cross-section view of the H-CST 8MR. H_2O Ow2 is in the center of the channels but outside of the 8MR, and Ow1 is along the walls of the channels. Color code: Ti (purple), Si (blue), O (red), and H (gray).

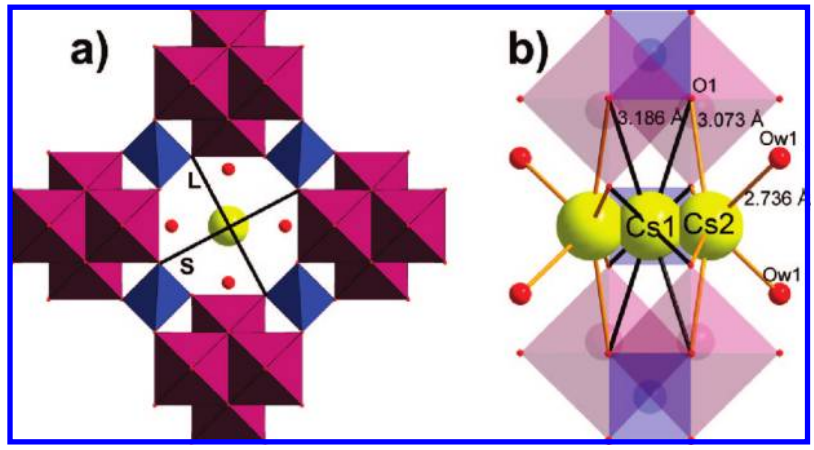

Figure 2. Polyhedral representation of the (Cs, H)-CST framework. (a) View down the (Cs, H)-CST 8MR along [001]. The channel dimensions are now equivalent, having L/S = 1. (b) Cross-section view of the (Cs, H)-CST 8MR window; Cs1 is located in the center and Cs2 outside of the 8MR window. Color code: Ti (purple), Si (blue), O (red), and Cs (yellow).

permanent storage of nuclear waste, the successful synthesis of those engineered materials requires an atomic-scale understanding and enhancement of their physicochemical properties based on molecular responses to the sequestration processes.

Sodium cations in the as-synthesized or native form of CST (Na-CST; $Na_2Ti_2SiO_7 \cdot 2H_2O$) can be ion-exchanged to form H-CST, and this material sequesters ^{137}Cs and ^{90}Sr from radioactive nuclear waste solutions.[4,5,9–16] Studies of the structures of CST in native and exchanged forms[4,17–19] immediately identified two sites in the structure for Cs exchange and noted that the H and Cs forms possess subtle differences in symmetry. Specifically, the H-CST framework possesses elliptical eight-membered-ring (8MR) channel openings (Figure 1) while the Cs form has circular ones (Figure 2). This observation led straightforwardly to the synthesis of Nb-substituted forms possessing circular openings, resulting in a quantitative improvement in ion selectivity.[20–22] Therefore, the framework is more than a formless box that simply carries the anionic charge that is balanced by the exchangeable cations. Although subtle, the conformational differences between the CST frameworks in H- and Cs-CST play a vital role in the way these materials select and capture Cs. Questions that have to date remained unanswered concern the ion-exchange paths for both Cs and H, the role of H_2O during the exchange process of hydrated ions, and the origin of the high ion selectivity in CST.

In materials that distort[23–26] to accommodate the exchanged ions, the mechanism of ion exchange is inherently time- and pathway-dependent, so structural studies targeting the mecha-

(9) Hritzko, B. J.; Walker, D. D.; Wang, N. H. L. *AIChE J.* **2000**, *46*, 552–564.
(10) Marinin, D. V.; Brown, G. N. *Waste Manage.* **2000**, *20*, 545–553.
(11) Zheng, Z.; Anthony, R. G.; Miller, J. E. *Ind. Eng. Chem. Res.* **1997**, *36*, 2427–2434.
(12) Anthony, R. G.; Dosch, R. G.; Gu, D.; Philip, C. V. *Ind. Eng. Chem. Res.* **1994**, *33*, 2702–2705.
(13) Sylwester, E. R.; Hudson, E. A.; Allen, P. G. *Geochim. Cosmochim. Acta* **2000**, *64*, 2431–2438.
(14) Anthony, R. G.; Philip, C. V.; Dosch, R. G. *Abstr. Pap.—Am. Chem. Soc.* **1992**, *203*, FUEL 37.
(15) Anthony, R. G.; Dosch, R. G.; Philip, C. V. U.S. Patent 6,110,378, 1995.
(16) Anthony, R. G.; Dosch, R. G.; Philip, C. V. U.S. Patent 6,479,427, 2002.
(17) Poojary, D. M.; Bortun, A. I.; Bortun, L. N.; Clearfield, A. *Inorg. Chem.* **1996**, *35*, 6131–6139.
(18) Medvedev, D. G.; Tripathi, A.; Clearfield, A.; Celestian, A. J.; Parise, J. B.; Hanson, J. *Chem. Mater.* **2004**, *16*, 3659–3666.
(19) Xu, H. W.; Navrotsky, A.; Nyman, M. D.; Nenoff, T. M. *J. Mater. Res.* **2000**, *15*, 815–823.
(20) Poojary, D. M.; Cahill, R. A.; Clearfield, A. *Chem. Mater.* **1994**, *6*, 2364–2368.
(21) Tripathi, A.; Medvedev, D. G.; Nyman, M.; Clearfield, A. *J. Solid State Chem.* **2003**, *175*, 72–83.
(22) Bortun, A. I.; Bortun, L. N.; Clearfield, A. *Solvent Extr. Ion Exch.* **1996**, *14*, 341–354.

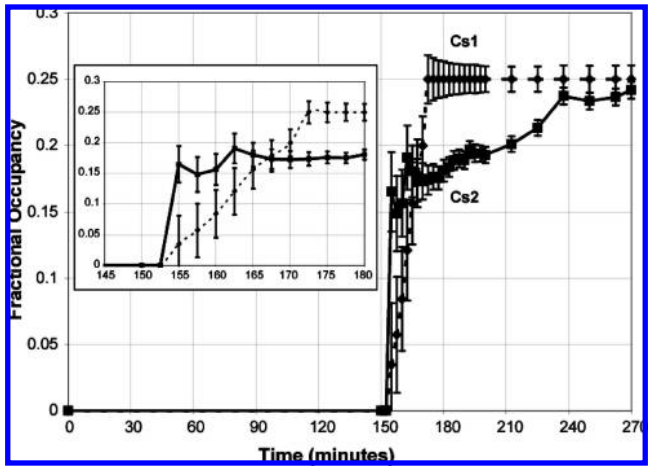

Figure 3. Results of the fractional Cs occupancy refinements for Cs1 and Cs2 during Cs^+ ion exchange into H-CST. The insert is a zoomed plot for the 145−180 min time range.

nism are best carried out using time-resolved diffraction techniques. However, only recently have the mechanisms and dynamics that control ion-diffusion processes in framework crystalline molecular sieves been studied with in situ diffraction techniques.[24,27,28] These time-resolved X-ray diffraction (TR-XRD) studies have revealed the sequence in which sites are exchanged, which in turn reveals the underlying mechanisms of ion selectivity in CST. These results demonstrate that the structural distortion responsible for ion selectivity and the conformational changes in the framework are mediated through a series of repulsive forces.[29] Water, which is always present, was not thought to be a significant participant in these processes.

A combination of in situ TR-XRD measurements sensitive to time-dependent changes in Cs^+ occupancies, plane-wave density functional theory (DFT) calculations, and time-resolved neutron powder diffraction (NPD) measurements sensitive to hydrogen (deuterium)[29] reveal a more complex and elegant mechanism that may well be operative in many other selective exchange processes. In situ time-resolved powder diffraction techniques, especially at neutron sources, involve significant compromises resulting from inherently poor counting statistics and signal-to-noise discrimination due to parasitic scattering from the ion-exchange media and environmental cells. The complementary information provided by X-rays, neutrons, and theory ameliorates this situation, especially when combined with accurate structure models for native and ion-exchanged phases.[29] These models, along with theoretical insights, serve to constrain structure refinements for models of the transient intermediate structural states that ultimately provide the time sequence and a frame-by-frame visualization of the exchange mechanism (see movies S1 and S2 described in the Figure 4 caption) and ion selectivity.

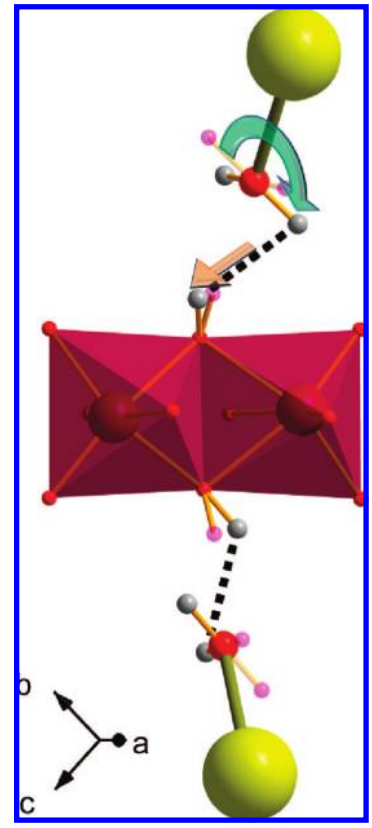

Figure 4. Illustration of the double-lever mechanism involving interactions of Cs2 with H_2O (Ow2) and hydroxyl, as calculated with DFT. Upon Cs^+ exchange, H_2O is forced to rotate close to the framework [lever 1 (green arrow)], and as a result, initiates lever 2 (orange arrow). The hydroxyl bends away from the approaching H_2O. Color code: Cs^+ (yellow), O^{2-} (red), Ti^{4+} (purple); transparent pink atoms are the H^+ positions in the H-CST form, and gray atoms are the H^+ positions in the (Cs, H)-CST form. The dashed line is the final H−H distance of 2.138(5) Å.

Ⓦ Movie S1 showing the correlation of the system energy with the operation of the double-lever mechanism and movie S2 showing the double-lever mechanism viewed in the [001] direction down the 8MR channel are available.

Methods and Materials

Preparation of Samples and Ion-Exchange Solutions. The starting material Na-CST [$a = b = 7.8060(1)$ Å, $c = 11.9599(2)$ Å, space group $P4_2/mcm$], which was first characterized by Poojary et al.,[20] was synthesized according to the procedures of Medvedev et al.[18] Starting gels of molar oxide composition $TiO_2/SiO_2/Na_2O$/deionized H_2O = 1.0:1.98:6.77:218 were prepared by first adding 6.6 mL of $TiCl_4$ to 23.30 mL of H_2O in a plastic bottle (A) of 500 mL capacity. To this mixture in bottle A, 40 mL of 30% H_2O_2 in H_2O was added, followed by 150 mL of deionized H_2O and 40 mL of 10 M NaOH solution. To a second 500 mL plastic bottle (B), 200 mL of 1 M NaOH and 4.3 g of colloidal silica (Ludox AS-40) were added, and then bottles A and B were combined in a single 500 mL plastic bottle. The pH of the final solution was adjusted by adding 1 M NaOH solution until a pH of 12.6−12.8 was achieved. The gel was not allowed to age but was immediately treated hydrothermally in 30 and 100 mL Teflon-lined stainless-steel Parr autoclaves at 210 °C for 10 days in a convection oven. The resulting white powder was filtered using a vacuum flask with 0.45 μm filter paper, rinsed with deionized water, and left to air-dry at room temperature. XRD data were collected on all of the synthesized samples and showed Na-CST to be the dominant phase.

(23) Bauer, T.; Baur, W. H. *Eur. J. Mineral.* **1998**, *10*, 133–147.
(24) Celestian, A. J.; Parise, J. B.; Goodell, C.; Tripathi, A.; Hanson, J. *Chem. Mater.* **2004**, *16*, 2244–2254.
(25) Nery, J. G.; Mascarenhas, Y. P.; Cheetham, A. K. *Microporous Mesoporous Mater.* **2003**, *57*, 229–248.
(26) Lee, Y. J.; Carr, S. W.; Parise, J. B. *Chem. Mater.* **1998**, *10*, 2561–2570.
(27) Celestian, A. J.; Medvedev, D. G.; Tripathi, A.; Parise, J. B.; Clearfield, A. *Nucl. Instrum. Methods Phys. Res., Sect. B* **2005**, *238*, 61–69.
(28) Parise, J. B.; Cahill, C.; Chen, J. *Abstr. Pap.—Am. Chem. Soc.* **1998**, *215*, U811.
(29) Celestian, A. J.; Parise, J. B.; Smith, R. I.; Toby, B. H.; Clearfield, A. *Inorg. Chem.* **2007**, *46*, 1081–1089.

A small amount of impurity phase was present in all of the preparations. The strongest peak from the impurity phase in the XRD patterns was <1% of the strongest peak from Na-CST. Diffraction peaks from the impurity phase could not be indexed on the basis of unit cells corresponding to known impurity phases such as sodium nonatitanate ($Na_4Ti_9O_{20}\cdot xH_2O$)[30] or sodium titanium oxide silicate (Na_2TiSiO_5).[31] Attempts to determine its unit cell parameters using standard powder-indexing software[32] were also unsuccessful. These extra peaks from the impurity phase did not change in position or intensity after ion exchange; from this observation, it was concluded that no Cs^+ ion exchange occurred in the impurity phase, and thus, this phase did not affect the total uptake of Cs^+ from solution.

For H-CST ion-exchange studies, the synthesized Na-CST was H^+-exchanged according to the methods described by Poojary et al.[17] in order to obtain H-CST [$a = b = 11.0690(6)$ Å, $c = 11.8842(6)$ Å, space group $P4_2/mbc$). Approximately 0.5 g of Na-CST was stirred in a 1 M HCl solution for 1 h. The powder was then filtered from the solution, and the structure and composition were verified by XRD and energy-dispersive spectroscopy, respectively, to possess the $P4_2/mbc$ structure and contain no Na^+.

Ion-exchange solutions were prepared at room temperature and ambient pressure. For Cs^+ exchange into H-CST, a 10 μM CsCl solution was used. Previous XRD studies had shown that initial uptake into H-CST was extremely rapid, and therefore, using a low-concentration solution would slow the ion-exchange process.

Ion-Exchange In Situ Flow-Through Cell. The in situ flow-through cell [see Supplementary Figure (SF) 1 in the Supporting Information] was designed in-house to maximize experimental flexibility, allow precise solution-flow control, and decrease the scattering contribution of the experimental cell to the diffraction pattern. A powdered sample was placed in the center of a 5.5 cm polyimide tube with an outer tube diameter of 1.5621 mm. The powder was held in place by glass wool on both sides that was supported by smaller sections (2 cm in length) of polyimide tubes with an outer diameter of 0.5461 mm. Flangeless ferrules with built-in 0.5 μm frits capped the larger polyimide tube. Solution flow rates were controlled with a peristaltic pump to maintain a drip rate of 2 drops/min.

X-ray Diffraction Methods. X-rays [$\lambda = 0.9223(1)$ Å] at the X7B beamline[33] of the National Synchrotron Light Source were used to probe the ion-exchange processes in real time. Diffracted intensities were collected on a MAR345 imaging plate (IP). Each diffraction pattern was collected for 1 min, with a 1.5 min lag time between diffraction patterns to read and erase the IP. The X7B goniometer is equipped with a rotating ϕ circle set at a fixed χ value of 90°. The sample was rotated ($\Delta\phi = 60°$) during data collection to help improve powder averaging and then moved back to the starting position before the next frame was acquired. At the end of each experiment, data from the IP were integrated to obtain 2θ-versus-intensity ASCII files using the program Fit2D.[34,35] The resulting one-dimensional (1D) diffraction patterns were used for unit cell and Rietveld structure refinements implemented in the programs Bruker-AXS Topas and WinPLOTR/FullProf.[36,37]

Refinement Strategies. The refinement of TR-XRD data proceeded in two steps. The first step consisted of full-pattern-decomposition Le Bail refinements[38] to obtain unit cell and profile parameters. The profile was modeled using a Thompson−Cox−Hastings pseudo-Voigt function,[39] whre the U, V, and W full width at half-maximum parameters and the X and Y shape parameters were refined. Once the calculated profile fit the experimental data with $\chi^2 < 1.25$, the profile parameters were fixed for all subsequent refinements. The unit cell parameters a and c were continuously refined. Each diffraction pattern had a unique background profile, which was fit using manually selected points and then interpolated using a cubic spline. The 2θ offset was refined to 0.0253(1)°.

Structure models for each phase were refined using the Rietveld method[40] in FullProf or Topas Academic in order to obtain occupancies and positions of extra framework cations. The framework atomic positions were not refined for the H-CST and (Cs, H)-CST exchange series since the unit cell parameters of those phases did not change within error. Fourier difference maps were calculated for all of the least-squares cycles and all of the phases during the refinement and were visualized/searched with the GFourier program.[41] Peaks found in the Fourier difference maps were then imported into the structure model, where their positions and occupancies were refined.

Computational Methods. The 3D periodic plane-wave DFT calculations were carried out using the Vienna Ab Initio Simulation Package (VASP).[42,43] The Perdew−Burke−Erzenhof form[44] of the generalized gradient approximation (GGA) was used for the electron correlation and exchange functionals. Projector-augmented wave pseudopotentials were used to describe the influence of the nuclear and core electrons on the valence-shell electrons. Small-core pseudopotentials were used for H (H_h), O (O_h), Ti (Ti_pv), Si (Si_h), and Cs (Cs_sv). Thus, 1, 6, 10, 4, and 9 electrons, respectively, were explicitly treated as valence electrons for these atom types. An energy cutoff of 800 eV was used for all of the energy minimizations with the "Accurate" precision level as defined in VASP. A precision level of "Low" was used in the molecular dynamics (MD) simulation, which was carried out for 250 time steps with a time step (Δt) of 1 fs. The Γ-centered Monkhorst−Pack[45] 2 × 2 × 2 grid was used for sampling the Brillouin zone. Convergence criteria for the energy minimizations were set to 1×10^{-4} eV and −0.02 eV/Å for the energy difference (EDIFF) and energy gradient (EDIFFG), respectively.

Initial atomic positions (including H^+) for the H-CST phase were taken from Celestian et al.[29] The Cs^+ positions in the $P4_2/mcm$ setting were transformed to the $P4_2/mbc$ setting and incorporated into the H-CST structure. The resulting structure model was converted to the $P1$ space group, and the calculations were performed on one unit cell with periodic boundary conditions. Three calculations were made to test how the H-CST crystal structure responded to the incorporated Cs^+ sites. The first tested how well the VASP code reproduced the starting H-CST structure. The second had only Cs^+ at site Cs2, and the third had only Cs^+ at site Cs1. All of the atoms were allowed to move except for those at the Cs^+ positions, which allowed the unit cell, framework sites, and extra-framework sites to move in response to the incorporated Cs^+. Trajectories and structures from VASP were analyzed within the wxDragon[46] software package.

(30) Yates, S. F.; Sylvester, P. *Sep. Sci. Technol.* **2001**, *36*, 867–883.
(31) Nyman, H.; Okeeffe, M.; Bovin, J. O. *Acta Crystallogr., Sect. B* **1978**, *34*, 905–906.
(32) Shirley, R. The Crysfire System for Automatic Powder Indexing, version 9.33; University of Surrey: Guildford, U.K., 2000.
(33) National Synchrotron Light Source; Vol. 2004, 2004; http://www.chemistry.bnl.gov/SciandTech/CRS/X7b/x7bhome.html.
(34) Hammersley, A. P. *FIT2D V9.129 Reference Manual V3.1*; ESRF: Grenoble, France, 1998.
(35) Hammersley, A. P.; Svensson, S. O.; Hanfland, M.; Finch, A. N.; Hausermann, D. *High Presure Res.* **1996**, *14*, 235–248.
(36) Roisnel, T.; Rodríguez-Carvajal, J. *Mater. Sci. Forum* **2001**, *378−381*, 118–123.
(37) Rodríguez-Carvajal, J. *Phys. B* **1993**, *192*, 55–69.
(38) Le Bail, A.; Duroy, H.; Fourquet, J. L. *Mater. Res. Bull.* **1998**, *23*, 447–452.
(39) Thompson, P.; Cox, D. E.; Hastings, J. B. *J. Appl. Crystallogr.* **1987**, *20*, 79–83.
(40) Rietveld, H. M. *J. Appl. Crystallogr.* **1969**, *2*, 65–71.
(41) Gonzalez-Platas, J.; Rodríguez-Carvajal, J. GFourier; 2005.
(42) Kresse, G.; Joubert, D. *Phys. Rev. B* **1999**, *59*, 1758–1775.
(43) Kresse, G.; Furthmuller, J. *Phys. Rev. B* **1996**, *54*, 11169–11186.
(44) Perdew, J. P.; Burke, K.; Ernzerhof, M. *Phys. Rev. Lett.* **1996**, *77*, 3865–3868.
(45) Monkhorst, H. J.; Pack, J. D. *Phys. Rev. B* **1976**, *13*, 5188–5192.
(46) Bernhard, E. wxDragon; 2006.

Results

Time-Resolved XRD. Rietveld structure refinement[40] of models with variable Cs^+ occupancies using TR-XRD data (see Figure 3 and SFs 2 and 5 in the Supporting Information) revealed that the Cs^+-for-H^+ ion exchange proceeds via a two-step process coincident with structural conformational changes. The first step involves Cs^+ exchange into site Cs2, which is located outside of the 8MR windows. The onset of filling of site Cs2 to a fractional occupancy of 0.16(2) was rapid, occurring within one diffraction pattern (one minute) at minute 155. The filling of site Cs2 occurred simultaneously with transformation of the crystal structure from space group $P4_2/mbc$ to space group $P4_2/mcm$; the diffraction pattern containing both of these phases persisted to the end of the experiment (see SF 3 in the Supporting Information). The occupancy of site Cs2 was constant for 20 min from minute 155 to 175 during the filling of site Cs1, which is located in the center of the 8MR window (Figure 3). After site Cs1 was filled to its maximum occupancy of 0.25(2), site Cs2 started to fill again and continued for an additional 220 min, reaching a maximum fractional occupancy of 0.24(1). The final chemical formula for the fully exchanged (Cs, H)-CST phase was calculated from these Rietveld structure refinements and previous studies[29] to be $Cs_{0.36}H_{1.64}SiTi_2O_7 \cdot H_2O$. Hydrogen and Cs^+ content had been refined from neutron diffraction data and were consistent with this study.[29] Unit cell refinements of the single and multiphase diffraction patterns (see SF 4 in the Supporting Information) indicated that no significant change in unit cell lengths had occurred within experimental error for either phase. The following unit cell parameters were determined by Rietveld analysis (see SF 4 in the Supporting Information): for H-CST ($P4_2/mbc$), $a = 11.0690(6)$ Å and $c = 11.8842(6)$ Å; for (Cs, H)-CST ($P4_2/mcm$), $a = 7.847(2)$ Å and $c = 11.9100(6)$ Å. Bond valence sums of Cs1 and Cs2 to framework O^{2-} were 1.06 v.u. and 1.10 v.u., respectively. The calculated profile matched the measured profile (see SF 5 in the Supporting Information) and converged, with best values of $R_{wp} = 2.21$, $R_p = 1.7$, $R_{bragg} = 2.40$, and GOF = 3.69 at the beginning of the experiment (containing only H-CST) and worst values of $R_{wp} = 6.88$, $R_p = 4.88$, $R_{bragg} = 7.14$, and GOF = 4.19 at the end of the experiment [containing only (Cs, H)-CST] (see the Supporting Information for crystallographic parameters).

DFT Calculations. The first DFT calculation was for the H-CST structure, to establish a baseline for calculations on the other compositions. Atomic positions of the modeled H-CST structure agreed well with the experimentally derived structure, with a maximum shift in atomic displacements of 0.2 Å. This type of discrepancy between analytical and computed O−H bond lengths is common.[47] The successful modeling of the H-CST structure established the viability of this method to reproduce experimental observations.

The second DFT calculation was performed for the case of Cs^+ exchanged at site Cs2 only. An energy minimization was carried out, and the resulting structure had the H_2O molecules in the wrong orientation compared to experiment. In order to test whether the structure was stuck in a local minimum, an MD simulation in VASP was performed for 250 steps ($\Delta t = 1$ fs) at 298 K. After step 166, the total energy dropped from −830 kcal/mol to a minimum of −834 kcal/mol (see movie S1 and SF 6 in the Supporting Information). At this point in the simulation, the H_2O and hydroxyl geometries had changed significantly (Figure 4). The H_2O sites rotated 159° to maximize the Cs−H distance as a result of repulsive forces, and the hydroxyl groups moved away in response to the close H−H repulsive force (see movies S1 and S2).

Consequently, it appeared that the first energy minimization had been in a local minimum and that a small input of kinetic energy was capable of overcoming the energy barrier to a lower-energy minimum. When a second energy-minimization calculation on the lower-energy structure obtained after the MD simulation was performed, the structural transformation from $P4_2/mbc$ to $P4_2/mcm$ was observed, and the total energy dropped to −835 kcal/mol. Symmetry searching for the final calculated structure from the energy minimization confirmed the $P4_2/mcm$ space group, which agrees with the experimental results (see the Supporting Information).

The third DFT calculation was made for the case of Cs^+ exchanged at site Cs1 only. The energy-minimization calculations performed in VASP required 51 steps to reach the required convergence. The total energy dropped slightly, from −805.3 to −805.4 kcal/mol. The H_2O rotations occurred for half of the total number of H_2O molecules in the unit cell, and the hydroxyl groups did not rotate. The structure transformed from the initial space group of $P4_2/mbc$ to $P2/m$, which was not observed experimentally.

Discussion

The results of the DFT calculations provide significant insight into the mechanism whereby H-CST ($P4_2/mbc$) transforms to the (Cs, H)-CST ($P4_2/mcm$) structure. These DFT results are consistent with recent results obtained by time-resolved and static in situ neutron diffraction studies (see SF7 and SF 8 in the Supporting Information).[29] The transformation was mediated through repulsive forces between the Cs^+ in the Cs2 site and the H^+ on H_2O site Ow2 located on the walls of the 8MR. Upon Cs^+ exchange, the H_2O site Ow2 must change orientation from pointing toward the center of the 8MR to pointing toward the walls of the channel (Figure 4 and movies S1 and S2). This process, which is necessary to rehydrate the Cs^+ from solution at site Cs2 and minimize the total energy of the structure, is the first lever of the exchange mechanism. As a consequence of the rotation of site Ow2, the H^+ sites approach to within 1.69 Å of the hydroxyl groups on the framework; the hydroxyl groups bend 0.55 Å away from their original position in response to the repulsive force induced by the approaching H^+. This hydroxyl bending, which is the second lever, is coincident with the rotation of the chains of octahedra parallel to [001].

The H_2O and hydroxyl dynamic interaction changes the Ti−O bond geometry of the TiO_6 octahedra. As a result, the entire column of TiO_6 octahedra rotates ∼5.8° and produces the circular 8MR openings (Figure 2). Once the 8MR possesses an L/S value of 1.00, the framework adopts the new space group $P4_2/mcm$. The transformation to $P4_2/mcm$ also results in new bonding environments for Cs^+ at site Cs1.

The DFT results suggest a mechanism that explains the site-occupancy preferences of Cs^+ exchanging into the H-CST structure and the speed of the transformation process. The TR-XRD results (see the Supporting Information) show that a Cs2 occupancy of ∼0.15 is needed in order to transform the $P4_2/mbc$ structure to $P4_2/mcm$. Once the transformation occurs, site Cs1 becomes available for occupancy and dominates the exchange process. When site Cs1 reaches a maximum occupancy of 0.25, site Cs2 gradually increases in occupancy until it achieves a Cs^+ occupancy of nearly 0.25. From the neutron diffraction studies,[29] slow uptake of Cs^+ at site Cs2 may be

(47) Kubicki, J. D.; Apitz, S. E. *Am. Mineral.* **1998**, *83*, 1054–1066.

explained by Cs^+ positional disorder with Ow2. As Cs^+ enters the structure at site Cs2, Cs^+ must displace H_2O (Ow2), and this diffusion process is slowed within the crowded 1D 8MR channels (Figure 2). The slow process of displacing H_2O by Cs^+ was hypothesized to be a result of the relatively strong H-bond interactions between H_2O and hydroxyl. In comparison with the previous Cs^+ exchange studies of Celestian et al.,[27] the rapid uptake of Cs^+ at site Cs2 at very low concentrations (10 μM) was still present. The transformation occurred in the MD simulations in ~75 fs, and therefore, it may not be possible to observe the initial Cs2 uptake and structure transition experimentally with the current technique.

Although the present study of ion-exchange processes are time-dependent, the normalized time dependence could not be quantified. Kinetic analysis would require normalizing for the effects of particle sizes and shapes as well as capillary packing density. Uniform particle sizes are needed in order to quantify the ion diffusion through the depth of a particle, which is dependent on the size (proportional to $1/r^2$) and shape of that particle.[48] Particle-size measurements were made using a scanning electron microscope and showed a large variation in crystallite sizes, which ranged from 0.05 to 2 μm. Grinding the crystals to obtain a uniform particle radius may not suffice, since the ground particles would have irregular shapes and therefore possess varying diffusion coefficients. Another parameter influencing the total time of the exchange process is the capillary packing density. The number of exchanging particles per unit volume illuminated by X-rays would change the absolute timing of the apparent exchange rates, given the same solution concentration and flow rate. Neither of the above caveats could be controlled during this study. The main objectives of this study were to determine the mechanisms of ion exchange and relative site-specific exchange occupancies, and neither appeared to be affected by the above conditions.

Conclusion

TR-XRD and DFT calculations have revealed the mechanisms involved during the structure transformation from H-CST to (Cs, H)-CST and, ultimately, the mechanisms responsible for the remarkable ion selectivity of CST for Cs. The results show a double-lever mechanism involving repulsive forces between Cs^+ and the H_2O dipole that cause the H_2O to rotate ~159° in order to rehydrate Cs^+ at site Cs2. The Cs^+ hydration effect forced the hydrogen of the H_2O close to the hydroxyl groups, and this process was labeled lever 1. In response to the approaching H_2O, the hydroxyl groups bent away and were displaced by 0.55 Å; this process was labeled lever 2. Hydroxyl bending caused the TiO_6 columns to rotate ~5.8° and adopt the $P4_2/mcm$ space group. The initial and final hydroxyl and H_2O positions were verified experimentally by Celestian et al.[29] The structural transformation made available a new site (labeled as site Cs1) for Cs^+ occupancy in the center of the 8MR. From these diffraction studies, the Cs^+ loading capacity and rate of exchange are high, suggesting that H-CST is well-suited for application in radioactive waste sequestration methods.

Acknowledgment. Support for this work was provided by the Center for Environmental and Materials Sciences (CEMS) funded through Grant NSF-CHE-0221934, and the work was also funded through NSF-DMR-0800415, the Department of Energy through DE-FG07-01ER63300, and Westinghouse Savannah River Technology Center. Research was carried out in part at the National Synchrotron Light Source, Brookhaven National Laboratory, which is supported by the U.S. Department of Energy, Division of Materials Sciences and Division of Chemical Sciences, under Contract DE-AC02-98CH10886. Computation was supported in part by the Materials Simulation Center, an MRSEC and MRI facility at Penn State, and the Center for Environmental Kinetics Analysis (CEKA), an NSF/DOE Environmental Molecular Sciences Institute.

Supporting Information Available: Crystallographic information file containing data for the refined and MD structures (CIF), structural description of the H-CST and (Cs, H)-CST structures, results of unit cell refinements, diagram of the flow-through experimental design, TR-XRD patterns with Rietveld refinement plots, time-resolved neutron diffraction data, and molecular dynamics energy-minimization graphs. This material is available free of charge via the Internet at http://pubs.acs.org.

(48) Helfferich, F. *Ion Exchange*; McGraw-Hill: New York, 1962.

JA801134A